Astron. Astrophys. 320, 696–704 (1997)

ASTRONOMY AND ASTROPHYSICS

The Piccinotti AGN sample observed in the ROSAT All-Sky Survey

N. Schartel[1,2,3], **M. Schmidt**[4], **H.H. Fink**[3], **G. Hasinger**[5], **and J. Trümper**[3]

[1] ESA, IUE Observatory, Vilspa, P.O.Box 50727, E-28080 Madrid, Spain
[2] Affiliated to the Astrophysics Division, Space Science Department, ESTEC
[3] Max-Planck-Institut für extraterrestrische Physik, D-85748 Garching, Germany
[4] California Institute of Technology, Henry M. Robinson Lab of Astrophysics, Pasadena, California 91125, USA
[5] Astrophysikalisches Institut Potsdam, An der Sternwarte 16, D-14482 Potsdam, Germany

Received 11 June 1996 / Accepted 5 September 1996

Abstract. The ROSAT All-Sky Survey observations of the complete hard X-ray selected Piccinotti AGN sample demonstrate that the soft X-ray spectra of almost none of the sample AGN can be simply represented by the power law extrapolated from the 2 - 10 keV range. A comparison of the soft X-ray spectra of the sample members with their medium energy continua measured with HEAO-1 and EXOSAT revealed that about half of the AGN in the sample are inrinsically absorbed. Furthermore, almost all sample AGN show excess fluxes in their soft X-ray emission. These features in the spectra of active galactic nuclei have an important impact on the interpretation of the cosmic soft X-ray background.

Key words: galaxies: active – galaxies: Seyfert – galaxies: quasars – X-rays: galaxies

1. Introduction

About 50 per cent of the X-ray sources detected in the ROSAT all-sky survey (RASS) are expected to be AGN, mostly quasars (Trümper, 1983; Voges, 1992). The soft X-ray spectra of bright RASS sources, which can be identified with known optical AGN on the basis of positional coincidence, show only weak evidence for absorption exceeding the column density of our own Galaxy. In a sample of 58 X-ray bright Seyfert 1 galaxies detected in the ROSAT survey (Walter & Fink, 1993) there is only one source with significant intrinsic absorption in its spectrum. Furthermore, the mean absorption derived from the X-ray spectra of 102 bright RASS quasars is consistent with the Galactic value (Schartel et al., 1996a). This result is confirmed by mean spectra obtained from stacking underexposed spectra taken at hundreds of QSO positions compiled from the Large Bright QSO Survey (Schartel, 1994; Schartel et al., 1996b, Green et al., 1995).

Send offprint requests to: N. Schartel

On the other hand, observations of AGN at medium energy X-rays up to 10 keV yielded a large number of intrinsically absorbed spectra (Turner & Pounds, 1989). Considering the absorption cross sections of relevant atoms of the interstellar medium (Morrison & McCammon, 1983) and the exponential attenuation of the observed X-ray flux the strong selection for intrinsically unabsorbed spectra in samples observed with ROSAT can easily be explained by the sensitivity range of about (0.1 -2.4)keV of the PSPC detector (Pfeffermann et al., 1987).

The knowledge of the distribution of the intrinsic absorbing column densities and of the mean shape of AGN spectra is fundamental for the understanding of the spectral properties of the extragalactic soft X-ray background radiation. ROSAT observations of the *Lockman Hole* revealed that a substantial fraction ($\approx$ 60 per cent) of the cosmic X-ray background up to 2 keV is caused by the emission of discrete resolved sources (Hasinger et al., 1991; Hasinger et al., 1993; Hasinger, 1994). The majority of optically identified X-ray sources in deeply exposed ROSAT sky fields consists of AGN (Shanks et al., 1991; Henry et al., 1993; Hasinger et al.,1993). Most recent models to explain the spectrum of the soft X-ray background comprise a mixture of evolving AGN with a wide distribution of absorbing column densities (e.g. Madau et al., 1993; Comastri et al., 1993). A direct way to determine this distribution of column densities and spectral shapes at soft X-rays is to study complete, hard X-ray selected AGN samples with ROSAT. The best studied hard X-ray selected AGN sample is that one established from the HEAO1 all-sky survey by Piccinotti et al. (1982).

2. The Piccinotti AGN sample

The HEAO 1 experiment A2 (Rothschild et al., 1979) performed a complete X-ray survey of 8.2 sr of the sky at $|b| < 20^o$ down to a limiting sensitivity of $\sim 3.1 \cdot 10^{-11}$ erg cm^{-2} s^{-1} in the (2 - 10)keV band. Among the 85 detected and identified sources there were 31 AGN. They form a complete hard X-ray selected sample consisting of 27 Seyfert 1 galaxies, three Seyfert 2 galaxies, and the quasar 3C 273 (Piccinotti et al., 1982; Grandi et

Table 1. The Piccinotti-AGN-Sample

Common Name	RA (1950.)	Dec (1950.)	Typ[a]	z	$N_{H\ (gal.)}$ $[10^{20}\ cm^{-2}]$
III Zw 2[b]	0:07:56.7	10:41:47	S1	0.0898	6.09 ± 0.30[b]
Mrk 1152[b]	1:11:21.8	-15:06:39	S1	0.052	1.67 ± 0.10[b]
NGC 526a[b]	1:21:37.3	-35:19:34	S1	0.0189	2.33 ± 0.12[b]
Fairall 9[b]	1:21:51.2	-59:03:59	S1	0.0461	3.12 ± 0.37
Mrk 590[b]	2:12:00.4	0:59:57	S1	0.0252	3.07 ± 0.15[b]
ESO 198[b]	2:36:41.0	-52:24:18	S1	0.045	3.08 ± 0.37
3C 120[b]	4:30:31.6	5:14:59	S1	0.033	12.32 ± 0.62[b]
3A 0557[c]	5:56:21.2	-38:20:15	S1	0.0344	3.35 ± 0.17[b]
H0917-074[c]	9:17:03.0	-7:22:57	S1	0.169	3.30 ± 0.40[b]
NGC 2992[b]	9:43:17.6	-14:05:43	S1(N)	0.0073	5.56 ± 0.28[b]
NGC 3227[b]	10:20:46.8	20:07:08	S1	0.0033	2.19 ± 0.26
NGC 3783[b]	11:36:33.0	-37:27:41	S1	0.0091	9.41 ± 1.13
NGC 4151[b]	12:08:01.0	39:41:02	S1	0.0033	1.95 ± 0.23
3C 273[b]	12:26:33.3	2:19:43	Q	0.158	1.81 ± 0.13
NGC 4593[b]	12:37:04.6	-5:04:11	S1	0.0090	1.97 ± 0.10[b]
MCG-6-30-15[b]	13:33:01.5	-34:02:30	S1	0.0078	4.06 ± 0.20[b]
IC 4329A[b]	13:46:27.9	-30:03:41	S1	0.0160	4.55 ± 0.23[b]
NGC 5506[b]	14:10:39.1	-2:58:27	S1(N)	0.0061	4.22 ± 0.21[b]
NGC 5548[b]	14:15:43.5	25:22:01	S1	0.0166	1.58 ± 0.19
IRAS 1832[d]	18:32:32.8	-59:26:39	S2	0.019	7.25 ± 0.87
ESO 103[b]	18:33:22.0	-65:28:18	S1	0.013	7.86 ± 0.94
H1846-786[c]	18:39:04.0	-78:35:02	S1	0.074	10.08 ± 0.12
ESO 141[b]	19:16:57.0	-58:45:52	S1	0.0368	5.08 ± 0.61
MKN 509[b]	20:41:26.2	-10:54:17	S1	0.0352	4.04 ± 0.48
NGC 7172[b]	21:59:07.2	-32:06:36	S2	0.0085	1.65 ± 0.10[b]
NGC 7213[b]	22:06:12.0	-47:25:00	S1	0.0053	2.01 ± 0.24
3C 445[b]	22:21:14.8	-2:21:26	S1	0.057	5.31 ± 0.64
NGC 7314[b]	22:33:00.2	-26:18:32	S1(N)	0.0048	1.45 ± 0.10[b]
NGC 7469[b]	23:00:44.4	8:36:16	S1	0.0167	4.82 ± 0.24[b]
MCG -2-58-22[b]	23:02:07.2	-8:57:20	S1	0.0475	3.60 ± 0.18
NGC 7582[b]	23:15:38.4	-42:38:38	S2(N)	0.0050	1.48 ± 0.10[b]

[a]: S1: Seyfert 1, S1(N): narrow line Seyfert 1, S2: Seyfert 2, Q: Quasar

[b]: Kotilainen et al., 1992
[c]: Turner and Pounds, 1989
[d]: Ward et al., 1988

al., 1992). Due to their different spectral behaviour all BL Lac objects were excluded for the purpose of this paper. The most common name of the sources, their celestial position, their spectral type, and their redshift are given in Table 1. Redshifts and spectral classification were taken from Kotilainen et al. (1992). Additionally, the absorbing Hydrogen equivalent column densities due to interstellar matter in our Galaxy towards the celestial positions of the sample sources are listed in the Table 1. The values given are based on 21 cm radio measurements evaluated by Elvis et al. (1989) and by Stark et al.(1992). A comparison of N_H values common in both lists yielded a distribution of normalized deviations with a width of 12 per cent (Schartel, 1994). Therefore we assume that 12 per cent is the relative error of the Galactic column densities.

3. X-ray observations

Most of the AGN in the Piccinotti sample have been observed several times at X-rays individually with different space borne experiments. Up to date, systematic X-ray studies of the sample, however, have been undertaken only with the data obtained with the HEAO-1 and EXOSAT satellites. A compilation of these data and the X-ray measurements with ROSAT during the all-sky survey will be presented in the next sections.

Table 2. Previous X-ray measurements

	HEAO 1 Measurements			EXOSAT Measurements				
Name	$CR_{A2}^{(a,b)}$	$F_{A2}^{(b,c,d)}$	$L_{A2}^{(b,c,e)}$	$\Gamma_{ME}^{(f)}$	$N_H^{(f,g)}$	$CR_{ME}^{(b,h,i)}$	$F_{cor.}^{(b,c)}$	$L_{cor.}^{(b,d)}$
III Zw 2	1.64 ± 0.24	$3.6^{(k)} \pm 0.5$	13.3 ± 1.9	$1.69^{+0.37}_{-1.20}$	$10^{+7.8}_{-2.1}$	1.80	3.43	12.74
Mrk 1152	1.49 ± 0.22	$3.2^{(k)} \pm 0.5$	3.9 ± 0.6	$1.93^{+0.36}_{-0.89}$	$3^{+2.0}_{-2.0}$	0.54	0.80	0.96
NGC 526a	2.52 ± 0.19	$5.5^{(k)} \pm 0.4$	0.9 ± 0.1	$1.55^{+0.11}_{-0.11}$	164^{+83}_{-83}	0.69	1.54	0.24
Fairall 9	1.29 ± 0.18	$2.8^{(k)} \pm 0.4$	2.7 ± 0.4	$1.96^{+0.26}_{-0.52}$	3^{+2}_{-1}	0.93	1.25	1.17
Mrk 590	1.34 ± 0.23	$2.9^{(k)} \pm 0.5$	0.8 ± 0.1	$1.92^{+0.25}_{-0.47}$	2^{+2}_{-1}	1.90	2.71	0.75
ESO 198	2.12 ± 0.14	$4.6^{(k)} \pm 0.3$	4.1 ± 0.3	$1.79^{+0.20}_{-0.48}$	3^{+1}_{-1}	1.35	2.01	1.80
3C 120	2.04 ± 0.25	$4.4^{(k)} \pm 0.5$	2.1 ± 0.3	$1.80^{+0.04}_{-0.06}$	13^{+2}_{-1}	2.43	4.36	2.08
3A 0557	1.36 ± 0.16	$3.0^{(k)} \pm 0.3$	1.5 ± 0.2	$1.37^{+0.23}_{-0.31}$	70^{+90}_{-40}	0.84	1.48	0.78
H0917-074	1.36 ± 0.28	$4.0^{(k)} \pm 0.6$	41.2 ± 8.5	$1.70^{(o)}$	≥ 3.3	≥ 0.56	≥ 0.80	≥ 1.11
NGC 2992	3.44 ± 0.25	$7.5^{(k)} \pm 0.5$	0.2 ± 0.2	$1.62^{+0.37}_{-0.52}$	68^{+22}_{-22}	1.50	2.87	0.07
NGC 3227	1.71 ± 0.24	$3.7^{(k)} \pm 0.5$	0.017 ± 0.002	$1.51^{+0.12}_{-0.12}$	11^{+6}_{-6}	1.85	2.73	0.01
NGC 3783	1.95 ± 0.23	$4.2^{(k)} \pm 0.5$	0.15 ± 0.02	$1.44^{+0.14}_{-0.19}$	11^{+8}_{-2}	2.74	4.84	0.17
NGC 4151	6.34 ± 0.26	$13.1^{(l)} \pm 0.5$	0.062 ± 0.003	$1.55^{+0.04}_{-0.04}$	900^{+80}_{-80}	12.0	31.93	0.15
3C 273	3.46 ± 0.26	$7.1^{(m)} \pm 0.5$	85.3 ± 6.4	$1.53^{+0.11}_{-0.06}$	3	5.23	8.32	102.80
NGC 4593	1.75 ± 0.26	$3.8^{(k)} \pm 0.6$	0.13 ± 0.02	$1.76^{+0.09}_{-0.19}$	2.3	2.32	3.51	0.12
MCG-6-30-15	2.12 ± 0.18	$4.6^{(k)} \pm 0.4$	0.12 ± 0.01	$1.69^{+0.14}_{-0.19}$	41^{+25}_{-31}	2.50	5.71	0.15
IC 4329A	3.70 ± 0.21	$8.0^{(k)} \pm 0.5$	0.90 ± 0.05	$1.75^{+0.09}_{-0.09}$	15^{+4}_{-3}	9.47	7.41	0.83
NGC 5506	2.69 ± 0.22	$5.9^{(k)} \pm 0.5$	0.094 ± 0.008	$1.84^{+0.04}_{-0.04}$	280^{+50}_{-50}	5.00	11.50	0.18
NGC 5548	2.92 ± 0.23	$6.4^{(k)} \pm 0.5$	0.76 ± 0.06	$1.58^{+0.07}_{-0.16}$	6^{+3}_{-3}	2.37	3.71	0.45
IRAS 1832	1.55 ± 0.21	$3.4^{(k)} \pm 0.5$	0.53 ± 0.07	$1.70^{(o)}$	≥ 7.3		$\geq 2.5^{(p)}$	≥ 0.4
ESO 103	1.36 ± 0.18	$3.0^{(k)} \pm 0.4$	0.22 ± 0.03	$1.92^{+0.34}_{-0.34}$	1350^{+330}_{-230}	1.04	4.90	0.36
H1846-786	1.33 ± 0.16	$2.9^{(k)} \pm 0.3$	7.2 ± 0.9	$3.50^{+1.70}_{-1.70}$	640^{+460}_{-300}	1.28	4.05	8.87
ESO 141	1.70 ± 0.17	$3.7^{(k)} \pm 0.4$	2.2 ± 0.2	$1.52^{+0.22}_{-0.40}$	12^{+2}_{-1}	1.77	2.93	1.77
MKN 509	2.08 ± 0.24	$4.5^{(k)} \pm 0.5$	2.5 ± 0.3	$1.86^{+0.10}_{-0.11}$	$3^{+1}_{-0.1}$	3.37	4.82	2.62
NGC 7172	2.00 ± 0.23	$5.1^{(n)} \pm 0.6$	0.16 ± 0.02	$1.84^{+0.49}_{-0.58}$	900^{+380}_{-300}	1.51	5.95	0.19
NGC 7213	1.07 ± 0.21	$2.3^{(k)} \pm 0.5$	0.028 ± 0.006	$1.85^{+0.09}_{-0.20}$	$1.5^{+0.5}_{-0.4}$	3.36	5.01	0.06
3C 445	1.55 ± 0.24	$3.4^{(k)} \pm 0.5$	4.9 ± 0.8	1.34	530^{+610}_{-370}	0.59	1.69	2.51
NGC 7314	1.39 ± 0.22	$3.0^{(k)} \pm 0.5$	0.030 ± 0.005	$1.78^{+0.49}_{-1.29}$	82^{+89}_{-9}	1.40	3.46	0.03
NGC 7469	1.77 ± 0.25	$3.9^{(k)} \pm 0.5$	0.47 ± 0.07	$1.78^{+0.08}_{-0.09}$	2^{+1}_{-1}	2.19	3.21	0.39
MCG -2-58-22	1.88 ± 0.25	$4.1^{(k)} \pm 0.5$	4.1 ± 0.5	$1.79^{+0.07}_{-0.12}$	$1.9^{+0.5}_{-0.4}$	4.29	6.41	6.42
NGC 7582	2.51 ± 0.23	$5.5^{(k)} \pm 0.5$	0.059 ± 0.005	$1.70^{(o)}$	1670^{+580}_{-490}	0.67	4.21	0.05

$^{(a)}$: R15 counts s^{-1}
$^{(b)}$: 1σ error
$^{(c)}$: for $2keV$—$10keV$
$^{(d)}$: 10^{-11} $erg\ cm^{-2}\ s^{-1}$
$^{(e)}$: 10^{44} $erg\ s^{-1}$
$^{(f)}$: 90 per cent confidence on multiparameter fit
$^{(g)}$: 10^{20} cm^{-2}
$^{(h)}$: for $2keV$—$6keV$
$^{(i)}$: $cts\ s^{-1}\ half\ s^{-1}$
$^{(j)}$: typical error is $\sim$ 10 per cent
$^{(k)}$: conversion factor: 2.175 10^{-11} $erg\ cm^{-2}$
$^{(l)}$: conversion factor: 2.070 10^{-11} $erg\ cm^{-2}$
$^{(m)}$: conversion factor: 2.040 10^{-11} $erg\ cm^{-2}$
$^{(n)}$: conversion factor: 2.570 10^{-11} $erg\ cm^{-2}$
$^{(o)}$: fixed at mean value
$^{(p)}$: based on Kotilainen et al., 1992

3.1. Measurements with HEAO-1

As mentioned above the complete AGN sample was formed from bright high galactic latitude X-ray sources discovered in the 2 -10 keV energy band with the A2 detectors aboard HEAO-1. Table 2 lists for each sample source the observed count rate, the 2 - 10 keV band flux, and the corresponding luminosity. The A2 count rate was taken from the first scan of the HEAO 1 mission in 1977 and 1978. It is given in R15-cts/s, a count rate which is combined of the rates registered by the MED and the HED detectors (Marshall et al., 1979). Adopting the "canonical" power law index Γ = 1.7, by which the medium energy X-ray continuum of almost all AGN observed with HEAO-1 is well described (Rothschild et al., 1983; Mushotzky, 1984), we used a conversion factor of $2.175 \cdot 10^{-11}$ erg cm^{-2} s^{-1} per R15-ct/s to calculate the 2 -10 keV fluxes. There are two exceptions: because of significant flatter continuums slopes we

Table 3. ROSAT All Sky Survey measurements and obtained fluxes

	Observation				**Fit**			**Fluxes**	
Name	Begin	End	T$^{(a)}$	$CR^{(b,d)}$	$N_{H_{intr.}}^{(c,d)}$	Γ	$\chi^2/d.o.f.$	$F^{(d,e,f)}$	$F_{cor.}^{(d,e,f)}$
III Zw 2	22-12-1990	24-12-1990	663	0.53 ± 0.04	$0.0^{+4.6}_{-0.0}$	1.4 ± 0.5	(HR)	1.10 ± 0.08	1.10 ± 0.08
Mrk 1152	14-01-1990	14-01-1991	621	1.02 ± 0.06	$0.4^{+1.1}_{-0.4}$	2.1 ± 0.4	0.97 / 11	1.28 ± 0.07	1.56 ± 0.08
NGC 526a	18-12-1990	20-12-1990	545	0.14 ± 0.03	$162.^{(h)}$	$2.36^{(i)}$		0.34 ± 0.07	7.10 ± 1.52
Fairall 9	25-11-1990	27-11-1990	550	3.67 ± 0.10	$0.0^{+0.4}_{-0.0}$	2.4 ± 0.3	1.27 / 15	8.07 ± 0.23	8.07 ± 0.23
Mrk 590	12-01-1991	14-01-1991	480	3.07 ± 0.10	$0.0^{+0.9}_{-0.0}$	2.3 ± 0.8	2.33 / 14	6.27 ± 0.21	6.27 ± 0.21
ESO 198	20-12-1990	24-12-1990	823	3.02 ± 0.08	$0.5^{+0.7}_{-0.5}$	2.5 ± 0.1	1.05 / 15	5.33 ± 0.13	7.45 ± 0.19
3C 120	19-08-1990	18-02-1991	793	2.19 ± 0.07	$28.^{+18.}_{-18.}$	3.2 ± 0.9	1.10 / 17	3.64 ± 0.11	72.1 ± 2.29
3A 0557	11-09-1990	14-09-1990	1031	0.14 ± 0.02	$66.7^{(g)}$	$2.36^{(i)}$		0.24 ± 0.03	2.27 ± 0.33
H0917-074	10-11-1990	12-11-1990	446	0.12 ± 0.03	$0.00^{(h)}$	$2.36^{(i)}$		0.27 ± 0.07	0.28 ± 0.67
NGC 2992	19-11-1990	21-11-1990	698	0.27 ± 0.03	$62.4^{(g)}$	$2.36^{(i)}$		0.47 ± 0.05	4.33 ± 0.47
NGC 3227	15-11-1990	17-11-1990	690	1.03 ± 0.02	$8.81^{(g)}$	$2.36^{(i)}$		1.45 ± 0.32	4.53 ± 1.00
NGC 3783	14-01-1991	15-01-1991	402	1.47 ± 0.08	$0.0^{+2.9}_{-0.0}$	2.7 ± 0.7	2.69 / 10	8.36 ± 0.45	8.36 ± 0.45
NGC 4151	29-11-1990	01-12-1990	665	0.65 ± 0.04	$0.1^{+1.2}_{-0.1}$	2.1 ± 0.4	1.19 / 10	0.92 ± 0.06	1.01 ± 0.06
3C 273	21-12-1990	23-12-1990	539	8.47 ± 0.16	$0.1^{+0.3}_{-0.1}$	2.3 ± 0.1	2.43 / 19	11.7 ± 0.22	12.7 ± 0.24
NGC 4593	15-07-1991	14-01-1991	181	3.48 ± 0.19	$0.3^{+0.9}_{-0.3}$	2.5 ± 0.2	1.18 / 9	4.81 ± 0.27	6.18 ± 0.34
MCG-6-30	19-01-1991	21-01-1991	447	3.63 ± 0.12	$1.6^{+1.1}_{-1.1}$	2.3 ± 0.2	1.14 / 11	6.32 ± 0.21	11.1 ± 0.37
IC 4329A	20-01-1991	21-01-1991	461	3.49 ± 0.12	$29.^{+21.}_{-21.}$	1.3 ± 0.8	0.66 / 14	6.18 ± 0.21	13.1 ± 0.44
NGC 5506	13-01-1991	18-01-1991	507	0.12 ± 0.06	$276.^{(g)}$	$2.36^{(i)}$		0.43 ± 0.09	17.3 ± 3.77
NGC 5548	02-01-1991	16-01-1991	658	5.48 ± 0.12	$0.5^{+0.4}_{-0.4}$	2.4 ± 0.1	2.81 / 18	6.40 ± 0.14	8.93 ± 0.19
IRAS 1832	18-09-1990	21-09-1990	224	0.26 ± 0.06	$0.0^{(h)}$	$2.36^{(i)}$		0.95 ± 0.23	0.95 ± 0.23
ESO 103	18-09-1990	19-09-1990	181	< 0.07	$1342.^{(g)}$	$2.36^{(i)}$		< 1.28	$< 3111.$
H1846-786	17-09-1990	19-09-1990	246	0.59 ± 0.07	$0.0^{+11.}_{-0.0}$	2.2 ± 0.8	(HR)	2.21 ± 0.25	2.21 ± 0.25
ESO 141	26-09-1990	28-09-1990	199	2.84 ± 0.16	$0.6^{+2.1}_{-0.6}$	2.3 ± 0.2	1.31 / 8	6.13 ± 0.34	8.56 ± 0.47
MKN 509	25-10-1990	27-10-1990	643	4.87 ± 0.12	$0.0^{+0.3}_{-0.0}$	2.3 ± 0.2	2.17 / 19	12.0 ± 0.28	12.0 ± 0.28
NGC 7172	06-11-1990	08-11-1990	473	< 0.04	$898.^{(g)}$	$2.36^{(i)}$		< 0.43	$< 228.$
NGC 7213	01-11-1990	02-11-1990	487	4.85 ± 0.13	$0.0^{+0.6}_{-0.0}$	2.0 ± 0.4	1.52 / 13	7.27 ± 0.19	7.27 ± 0.19
3C 445	22-11-1990	24-11-1990	447	< 0.03	$525.^{(g)}$	$2.36^{(i)}$		< 0.19	< 24.0
NGC 7314	16-11-1990	18-11-1990	416	0.35 ± 0.05	$81.^{(g)}$	$2.36^{(i)}$		0.61 ± 0.08	6.81 ± 0.93
NGC 7469	06-12-1990	08-12-1990	674	2.05 ± 0.07	$0.6^{+1.2}_{-0.6}$	2.4 ± 0.1	0.97 / 8	4.48 ± 0.16	6.58 ± 0.23
MCG-2-58	29-11-1990	01-12-1990	461	2.03 ± 0.09	$0.0^{+0.9}_{-0.0}$	1.9 ± 0.4	1.18 / 8	4.03 ± 0.17	4.02 ± 0.17
NGC 7582	17-11-1990	19-11-1990	255	< 0.05	$1669.^{(g)}$	$2.36^{(i)}$		< 1.19	$< 8396.$

$^{(a)}$: in s $^{(d)}$: 1σ error $^{(g)}$: from EXOSAT
$^{(b)}$: in s^{-1} $^{(e)}$: for 0.1 keV—2.4 keV $^{(h)}$: galactic absorption is assumed
$^{(c)}$: in 10^{20} cm^{-2} $^{(f)}$: in 10^{-11} $erg\ cm^{-2}\ s^{-1}$ $^{(i)}$: mean value for ROSAT spectra

applied for NGC4151 and for 3C 273 the conversion factors of 2.07 and $2.04 \cdot 10^{-11}$ erg cm^{-2} s^{-1} per R15-ct/s, respectively, as has already been supposed by Piccinotti et al.. The 2 - 10 keV luminosity is calculated according to Weinberg (1972) using H_o = 50 km s^{-1} Mpc^{-1} and q_o = 0.5. It is, furthermore, *k*-corrected according to Schmidt & Green (1986).

3.2. Measurements with EXOSAT

In the course of the years 1983 to 1986 the AGN of the Piccinotti sample were all studied with the Low Energy (LE) and the Medium Energy (ME) Experiments aboard EXOSAT (Turner & Pounds, 1989; Grandi et al., 1992), which are effectively sensitive in the energy bands (0.05 - 2)keV and (2 - 50)keV, respectively. The statistical significance of the measured X-ray spectra was high enough for most of the sample sources to allow the modelling of the count rate spectra with simple absorbed power laws by means of least squares fits. According to Turner & Pounds (1989) the determination of the absorbing column density needed to consider the data of both experiments, the LE and ME detectors. Subsequently, the obtained N_H value was used as a fixed parameter in power law fits to the ME data to determine normalization and photon index of the medium energy spectrum only. In addition to the HEAO-1 data Table 2 contains the following EXOSAT results: the best fit parameters Γ_{ME} and N_H together with the 2 - 6 keV ME count rate, the 2 - 10 keV band flux corrected for N_H, and the corresponding luminosity.

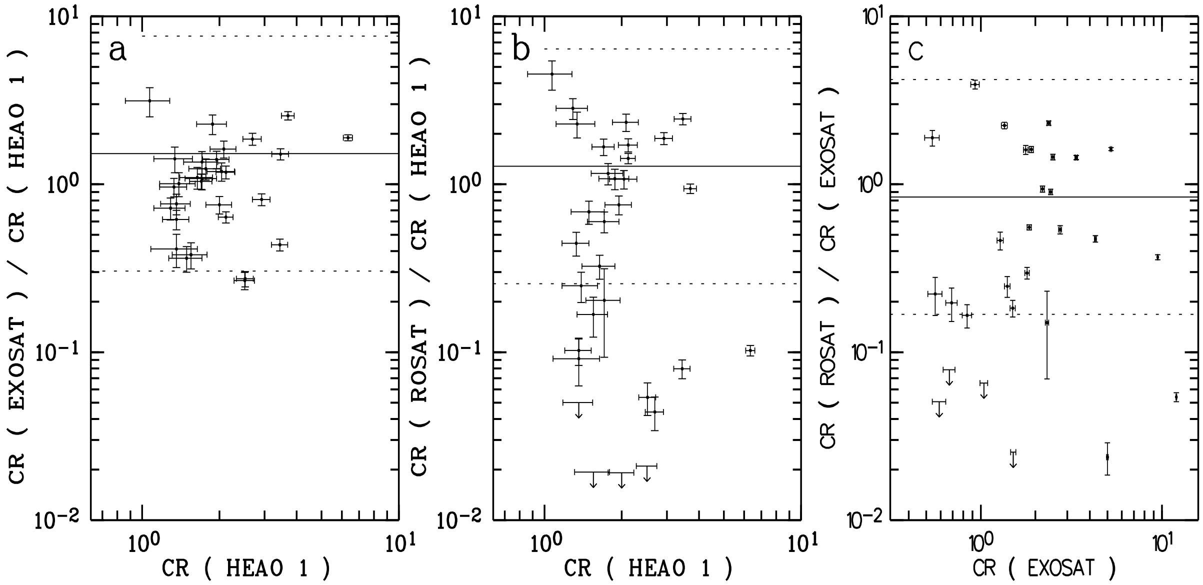

Fig. 1a–c. Ratio of count rates of AGN of the Piccinotti sample measured with HEAO-1, EXOSAT and ROSAT. **a** ratio of HEAO-1/A2 and EXOSAT/ME-Argon count rates as a function of the A2 count rate. The solid line represents the ratio expected for a medium energy power law continuum with an photon index of 1.7 and an average absorbing column density of $3 \cdot 10^{20}$ cm^{-2}. The dotted lines indicate the limits of the expected variability range. **b** ratio of ROSAT/PSPC and HEAO-1/A2 count rates as a function of the A2 count rate. **c** ratio of ROSAT/PSPC and EXOSAT/ME-Argon count rate as a function of the ME count rate.

3.3. ROSAT survey observations

The X-ray observations during the ROSAT all-sky survey (RASS) in 1990 and early 1991 were performed with the PSPC in the focal plane of the X-ray telescope. The extraction of spectral characteristics from X-ray point source images is described in Schartel et al. (1996). The results of the data reduction are binned pulse height spectra corrected for dead time, vignetting, and shadowing caused by the supporting structure of the PSPC's entrance window. In Table 3 the observation log, the total exposure, and the corrected count rate are listed for each of the sample sources.

For 17 sources of the Piccinotti sample the table contains the spectral parameters which resulted from least squares fits of absorbed power laws to the count rate spectra. That part of the total absorbing column density, which is caused by interstellar matter in the Milky Way, $N_{H\mathrm{gal}}$, is fixed in the fits. On the other hand, the absorption $N_{H\mathrm{intr}} = N_{H\mathrm{tot}} - N_{H\mathrm{gal}}$, intrinsic to the sources, is a free fit parameter. The errors quoted correspond to a 68.3% confidence level for three free parameters. With the best fit parameters we calculated the 0.1 - 2.4 keV fluxes using the corrected count rates. The table contains two flux values: the flux F is corrected for the Galactic absorption only, whereas the flux F_{cor} is corrected for the total absorption, i.e. for the Galactic column density towards the source considered and for that one intrinsic to it. The flux errors given are based on the statistical errors of the measured count rates and do not comprise any systematic uncertainties which can amount up to 4 per cent (RUH, 1994).

Four sources of the Piccinotti sample were not detected in the RASS. 3σ upper limits of their count rates and fluxes are given in the table. Eight further AGN were detected in the RASS just above the detection threshold. To estimate their fluxes in ROSAT's energy band we adopted the N_H values derived from the EXOSAT spectra and applied a power law index of $< \Gamma >= 2.36$ which revealed to be the mean index resulting from fits of the spectra of sample sources with sufficiently high photon statistics. The images of two additional sample AGN, which were definitely detected in the survey, contained too few counts to allow for a significant least squares fit. To estimate their spectral characteristics we employed a method based on hardness ratios which was developed by Schartel (1994) and which is described in detail by Schartel et al.(1996a).

4. Comparison of count rates

The non-detection of AGN in the ROSAT all-sky survey may be due either to intrinsic variability or photoelectric absorption. In order to estimate the influence of variability we compare the count rates of the Piccinotti sources as measured with HEAO-1 and EXOSAT. In Fig.1a the ratio of the HEAO-1/A2 R15 count rate and that one measured by the EXOSAT/Argon detector is given as a function of the source strength in units of A2 R15 cts/s for all sample sources. The observations of the same individual sources with HEAO-1 and EXOSAT are separated on average by 7 years. The data points scatter by a maximum factor of 12 independently of the source strength.

Firstly we have to ensure that this scatter is not induced by the different responses of both experiments to sources

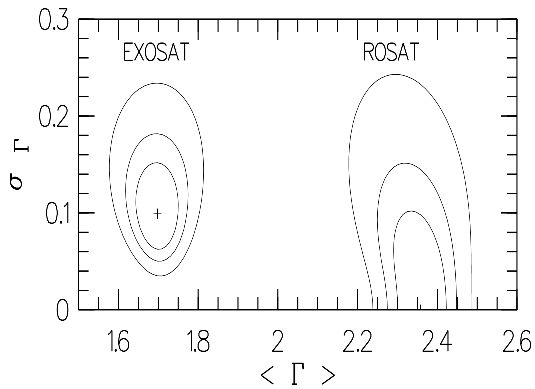

Fig. 2. Significance contour diagrams of the mean and the width of those photon index distributions of the X-ray spectra measured with both instruments, ROSAT and EXOSAT, in the energy bands 0.1 - 2.4 keV and 2 - 6 keV, respectively. The contours for the 68.3%, 90%, and 99% confidence levels are given.

spectra with a wide distribution of slopes. For this purpose we calculated the range of count rate factors CR(A2-R15)/CR(EXOSAT/Argon) for photon indices ranging from 1.3 to 2.0, the extrema of the EXOSAT spectra of the sample AGN (see Table 2). The absorbing column density was fixed to an average value of $N_H = 3 \cdot 10^{20}$ cm^{-2}. The differences in the conversion factors amount to at most 10 per cent, thus demonstrating that the scatter in Fig.1a is almost not affected by instrumental effects.

Next we compare the scatter of the count rate factor with the variability range found by Grandi et al. (1992) for the Piccinotti AGN sample as observed with the ME detectors abaord EXOSAT during the three years the satellite was active. The sources varied up to a factor of five over the observational interval. Some sources got brighter, others fainter in the course of the years. The total width of the variability range at medium photon energies is therefore given by a factor of about ten. This agrees well with the width of the scatter in Fig.1a. We therefore conclude that the observed fluctuations of the count rate ratio are mainly caused by variations of the medium energy X-ray emission of the Piccinotti AGN and that the ratio is hardly affected by low energy absorption.

If we consider the ratio of the count rate measured in the 0.1 - 2.4 keV energy band of ROSAT and that obtained at medium energies an asymmetric distribution is expected. Due to the sensitivity of ROSAT spectra to low energy absorption the count rate ratio CR(ROSAT)/CR(MED) of some sources with a large column densities along the line of might be very small, as it is shown in Fig.1b and Fig.1c.

5. The shape of the spectra

For a source radiating at a time a soft X-ray flux higher than that one expected by extrapolating the hard X-ray spectrum, measured at another instance of time, it cannot be *a priori* decided whether the soft excess flux is of due to differences in the assumed spectrum or due to intensity variations. A spectral origin of a supposed excess flux can be tested by comparing the means of power law indices determined in the soft and in hard X-ray energy band, respectively. For measurements with sufficient photon statistics the shape of the soft spectrum can be tested against more sophisticated model spectra.

5.1. Mean spectral behaviour

The photon statistics of the spectra of most of the Piccinotti sample AGN obtained during the HEAO-1 mission with the A2 experiment is too poor to allow the determination of spectral parameters. By using also the hard X-ray experiments abaord HEAO-1 Rothschild et al. (1983) found that the medium and hard energy spectra can be well described by a power law with a mean photon index of $\Gamma = 1.62 \pm 0.04$. Surprisingly, the dispersion of the index distribution was very small ($\Delta\Gamma \leq 0.15$). This result was confirmed by Mushotzky (1984) who found a mean index of $\Gamma = 1.68 \pm 0.15$ for broad line active nuclei.

In the case of EXOSAT measurements the statistically improved count rate spectra of 27 of the sample sources allowed the determination of simple fit parameters as photon index and absorbing column density. In order to obtain a sample mean and to get some ideas of the width of the index distribution we applied a maximum likelihood method developed by Maccacaro et al. (1988) which yielded:

$$< \Gamma_{\rm EXOSAT}(27) >= 1.70 \pm 0.03 \text{ and } \sigma_{\Gamma_{\rm EXOSAT}} = 0.10 \pm 0.03$$

The corresponding significance contours are given in Fig.2. The EXOSAT measurements are in excellent agreement with the HEAO-1 observations. In particular, they confirm the narrowness of the distribution of continuum slopes at medium energy X-rays.

Due to strong absorption at low photon energies only for 19 members of the Piccinotti sample enough ROSAT/PSPC counts could be accumulated to allow us to establish reliable soft X-ray spectra. The mean and the width of their index distribution are

$$< \Gamma_{\rm ROSAT}(19) >= 2.36 \pm 0.04 \text{ and } \sigma_{\rm ROSAT} < 0.07$$

The significance contours can be found in Fig.2. We conclude that the sample means of the power law indices as well as the width of their distribution is distinctly different in the soft and in the hard X-ray band, respectively (confidence level > 99%). To rule out a selection effect in favour of spectra with particularly high slopes, we calculate the EXOSAT mean for those 19 sample AGN, for which the ROSAT survey measurements yielded reliable count rate spectra.

$$< \Gamma_{\rm EXOSAT}(19) >= 1.70 \pm 0.04 \text{ and}$$

$$\sigma_{\Gamma_{\rm EXOSAT}}(19) = 0.09 \pm 0.03$$

This finding excludes possible selection effects and confirms the distinctness of the index distributions at different X-ray bands. Actually, 17 of the 19 sources observed significantly

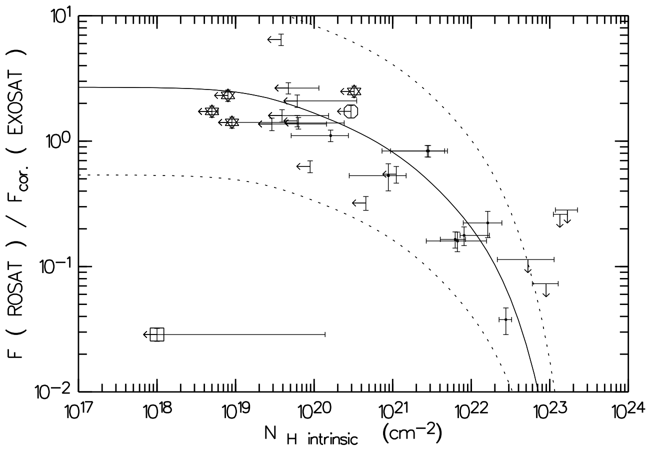

Fig. 3. Ratio of the soft X-ray flux measured with ROSAT and corrected for Galactic absorption and the medium energy flux measured with EXOSAT and corrected for the total absorption as a function of the intrinsic absorption defined as the difference between the total and the Galactic absorption towards the target source. The solid line represents the ratio for an average broken power law spectrum with a photon index of 1.7 above 2 keV and 2.36 at soft X-rays and with a fixed normalization at 2 keV. The dotted lines indicate the limits of the variability range. The star symbols mark sources whose spectra show evidence for a soft excess. NGC 3783 is symbolized by the circle and the square represents NGC 4151.

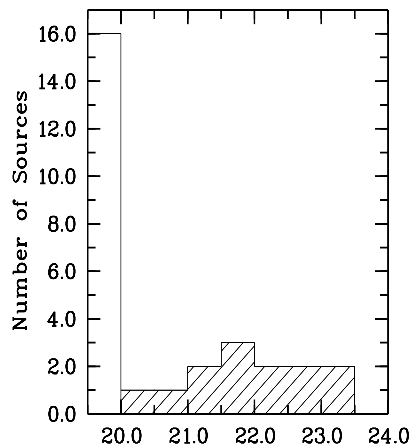

Fig. 4. Histogram of the intrinsic absorbing column densities observed with ROSAT for the AGN of the Piccinotti sample. AGN in the hatched area are interpreted as intrinsically absorbed sources.

during the ROSAT survey show higher indices of the continuum in the (0.1 - 2.4)keV band than beyond 2 keV (see Table 2 and Table 3). Especially, for weak and highly absorbed sources the index of the power law is very badly constrained, since the index and the column density are fitted simultanously. Both sources showing a flatter low-energy spectrum also have a high absorbing column density, either Galactic (II Zw 2 with $N_{H_{gal.}} = 6.01 \pm 0.3\ 10^{20}\ cm^{-2}$) or an intrinsic one (IC 4329A with $N_H = 29. \pm 21\ 10^{20}\ cm^{-2}$).

The fact that almost all AGN of the Piccinotti sample, which do not show strong intrinsic absorption, exhibit a steeper spectrum at soft than at hard X-rays is commonly interpreted as a soft X-ray flux excess, the origin of which is still under debate (Wilkes & Elvis, 1987; Turner & Pounds, 1989; Walter & Fink, 1993; Brinkmann et al., 1993; Fiore et al., 1994; Laor et al., 1994; Schartel et al., 1996a). ROSAT spectra of AGN with a superb photon statistics have been successfully represented by two-component models consisting of a power law above 1 keV and a steep, probably thermal component dominant at low photon energies (Walter et al., 1994; Molendi and Maccacaro, 1994; Pounds et al., 1994; Fink et al., 1996).

5.2. Intrinsic absorption

As we have seen above, the large range of count rates found in the RASS for the low energy spectra of the Piccinotti sample AGN cannot be explained either by variability or by spectral behaviour or by Galactic absorption only. It is therefore most probably that intrinsic absorption is responsible for the extent of the count rate ratio distribution. For 29 EXOSAT sources the absorbing column density could be determined from fits of simple absorbed power laws to the observed count rate spectra. These values were now used to calculate the absorption corrected (2 -10)keV fluxes F_{cor}(EXOSAT) adopting a continuum slope of $\Gamma = 1.70$. On the other hand, soft X-ray band fluxes F(ROSAT) corrected for Galactic absorption only have been derived from the ROSAT spectra assuming $\Gamma = 2.36$. In Fig.3 both flux values are compared for 29 sources of the Piccinotti sample as a function of the intrinsic absorption. For 19 samples sources the latter is derived from the total absorbing column densities resulting from fits to the ROSAT spectra. For the remaining ten AGN, for which the ROSAT measurements are statistically not appropriate, the N_H values of the EXOSAT fits were adopted. The dotted lines indicate again the range of expected variability. With the exception of NGC 4151 only four sources are located outside the variability range. For these sources only upper limits can be set. NGC 4151 is a special case. A detailed study of the EXOSAT measurement of this source revealed the existence of a partial absorber on the line of sight, the optical depth of which is variable in time (Yaqoob et al., 1989).

The combination of ROSAT/RASS and EXOSAT observations makes it possible to determine the fraction of AGN in the complete Piccinotti sample showing intrinsic absorption to 44.8 % (13 sources). In Fig.4 a histogram of the observed intrinsic column densities is given. In summary, about 50% of the members of the hard X-ray selected sample exhibit intrinsic absorption, which represents the most important selection effect for the statistical significance of point source detections in the ROSAT survey.

5.3. Warm absorber

Besides NGC 4151, for which, as mentioned above, partial absorption along the line of sight has been measured, recent studies revealed Turner et al., (1993) that the X-ray spectrum of a further sample source, NGC 3783, is affected not only by low energy

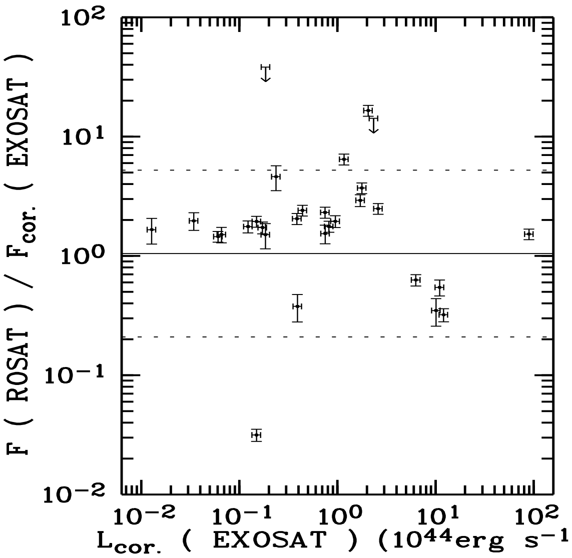

Fig. 5. Ratio of the absorption corrected fluxes measured with ROSAT/PSPC and EXOSAT/ME as a function of the medium energy X-ray luminosity. The solid line represents the ratio expected for a medium energy power law continuum with an photon index of 1.7 and the dotted lines indicate the limits of the expected variability range. Two further upper-limits are located above the plotted scale.

absorption due to cold matter, but also by the effects of intervening ionized matter which produces an absorption edge in the soft X-ray continuum below 1 keV. By fitting the ROSAT count rate spectra of this source obtained during the survey and at the occasion of a pointed observation we are able to confirm that an absorption edge near 0.8 keV improves the fit appreciably.

The conclusion that the ROSAT spectra of several sample AGN are weakened by an absorbing column density exceeding the Galactic value can finally be checked by considering instead the ratio of fluxes in soft and medium energy bands which have been corrected for any absorption. As can be seen from Fig.5 the majority of flux ratios are located within the limits of the variability range. It should be noted that their distribution is asymmetric in favour of ratios greater than that one of the representative spectrum. A fraction of 76.9% of the sources show a ratio greater than expected by interpolation from the medium energy band. This indicates that the absorption corrected soft X-ray fluxes of most of the sample sources are higher than those extrapolated from the medium energy power law spectrum, i.e. their soft X-ray spectra show soft X-ray excesses.

6. Conclusions

The Piccinotti sample is the best studied complete hard X-ray selected sample of nearby AGN. For the understanding of the bulk properties of AGN the investigation of the sample at different wavelengths is of special importance. We studied the sample at soft X-rays in the energy band (0.1 - 2.4)keV using measurements of the sources' count rate spectra obtained during the ROSAT all-sky survey in 1990/91. 27 out of the 31 sample AGN were detected in the survey showing a large range of count rates. A comparison of the soft X-ray ROSAT observations with (2 - 10)keV medium energy measurements performed with detectors aboard HEAO-1 and EXOSAT confirmed that a rather large fraction of the sources ($\approx 50\%$) show intrinsic absorption in their soft X-ray spectra. Furthermore, the comparison with hard X-ray spectra demonstrate that soft X-ray excesses are quite common. These spectral features of the X-ray emission of active galactic nuclei are most important for the interpretation of the cosmic soft X-ray background which is thought to be dominated by the emission of AGN.

Acknowledgements. The ROSAT mission was supported by the Ministerium für Bildung, Wissenschaft, Forschung und Technologie and by the Max-Planck Society. We thank the SASS and the EXSAS teams for processing the ROSAT survey data and for providing software for the data reduction. The subject of the present paper is part of the Ph.D.Thesis of N.S. who acknowledges a Max-Planck fellowship. M.S. thanks the Humboldt foundation for financial support.

References

Brinkmann W., Siebert J., Boller T., 1993, A& A **281**, 281
Comastri A., Setti G.-C., Zamorani G., Hasinger G., 1993, A& A **296**, 1
Elvis M., Lockman F.J., Wilkes B.J., 1989, AJ 97, 777
Fink H.H., Walter R., Schartel N., Engels D., 1996, A& A, accepted
Fiore F., Elvis M., McDowell J.C., et al., 1994, ApJ Suppl. 95, 1
Grandi P., Tagliaferri G., Giommi P., Barr P., Palumbo G.G.C., 1992, ApJS 82, 93
Green P.J., Schartel N., Anderson S.F., et al., 1995, ApJ 450, 51
Hasinger G., Schmidt M., Trümper J., 1991, A&A 246, L2
Hasinger G., Burg R., Giacconi R., et al., 1993, A&A 275, 1
Hasinger G., 1994, The Extragalactic X-Ray Background: ROSAT Observations, in: Warmsteker W., Longair M., Kondo Y.(eds.) Frontiers of Space and Ground-Based Astronomy: The Astronomy of the 21st Century. Kluwer Academic Publ., Dordrecht, 381
Henry J.P., Gioia I.M., Böhringer H., et al., 1993, ApJ **107**, 1270
Kotilainen J.K., Ward M.J., Boisson C., et al., 1992, MNRAS 256, 125
Laor A., Fiore F., Elvis M., Wilkes B.J., McDowell J.C., 1994, ApJ 435, 611
Maccacaro T., Gioia I.M., Wolter A., Zamorani G., Stocke J.T., 1988, ApJ 326, 680
Madau P, Ghisellini G., Fabian A.C., 1993, ApJ 410, L7
Marshall F.E., Boldt E.A., Holt S.S., et al. 1979, ApJS 40, 657
Molendi S., Maccacaro T., 1994, A & A **291**, 420
Morrison R., McCammon D., 1983, ApJ 270, 119
Mushotzky R.F., 1984, Adv.Space Res. 3, 157
Pfeffermann, E., Briel, U.G., Hippmann, H. et al. , 1987, MPE print 81
Piccinotti G., Mushotzky R.F., Boldt E.A., et al., 1982, ApJ 269, 423
Pounds K.A., Nandra K., Fink H.H., Makino F., 1994, MNRAS 267, 193
Rothschild R., 1979, Space Sci. Instr. 4, 265
Rothschild R., Mushotzky R.F., Baity W.A., et al., 1983, ApJ 269, 423
RUH: ROSAT Users' Handbook (Draft 1), 1994. www: *http : //ftp.rosat.mpe-garching.mpg.de/rosat_svc/doc/handbook/*
Schartel N., 1994, Ph.D. Thesis, Ludwig-Maximilians Universität, München
Schartel N., Walter R., Fink H.H., Trümper J., 1996a, A&A 307, 33

Schartel N., Green P.J., Fink H.H., et al., 1996b, MNRAS, accepted
Schmidt M., Green R.F., 1986, ApJ 305, 62
Shanks T., Georgantopoulos I., Stewart G.C., et al., 1991, Nat 353, 315
Stark A. A., Gammie C. F., Wilson R. W., 1992, ApJ Suppl., **79**, 77
Turner T.J., Pounds K.A., 1989, MNRAS 240, 833
Turner T.J., NANDRA K., GEORGE I., FABIAN A. C., POUNDS K. A., 1993 ApJ **419**, 127
Trümper J., 1983, Adv.Space Res. 2, 241
Voges W., 1992, The ROSAT All-Sky X-Ray Survey. In: Guyenne T.D., Hunt J.J. (eds.) Spaces Science with particular emphasis on High-Energy Astrophysics. ESA ISY-3, 9
Walter R., Fink H.H., 1993, A&A 274, 105
Walter R., Orr A., Courvoisier T.J.-L., et al., 1994, A & A 285, 119
Ward M. J., Done C., Fabian A. C., et al., 1988, ApJ **324**, 767
Weinberg S., 1972, Gravitation and Cosmology. John Wiley & Sons, New York
Wilkes B.J., Elvis M., 1987, ApJ 323, 243
Yacoob T., Warwick R.S., Pounds K.A., 1989, MNRAS 236, 153

This article was processed by the author using Springer-Verlag LaTeX A&A style file *L-AA* version 3.